The Journal of Prevention of Alzheimer's Disease 12 (2025) 100037

Contents lists available at ScienceDirect

The Journal of Prevention of Alzheimer's Disease

journal homepage: www.elsevier.com/locate/tjpad

Original Article

Microstructural white matter injury contributes to cognitive decline: Besides amyloid and tau

He-Ying Hu[b,1], Hong-Qi Li[a,1], Wei-Kang Gong[c,1], Shu-Yi Huang[a], Yan Fu[b], Hao Hu[b], Qiang Dong[a], Wei Cheng[c], Lan Tan[b,*], Mei Cui[a,*], Jin-Tai Yu[a,*]

[a] Department of Neurology and National Center for Neurological Disorders, Huashan Hospital, State Key Laboratory of Medical Neurobiology and MOE Frontiers Center for Brain Science, Shanghai Medical College, Fudan University, Shanghai, PR China
[b] Department of Neurology, Qingdao Municipal Hospital, Qingdao University, Qingdao, PR China
[c] Institute of Science and Technology for Brain-inspired Intelligence, Fudan University, Shanghai, PR China

ARTICLE INFO

Keywords:
Alzheimer's disease
White matter
Peak width of skeletonized mean diffusivity
Cognitive decline
Biomarker

ABSTRACT

Background: Cognitive decline and the progression to Alzheimer's disease (AD) are traditionally associated with amyloid-beta (Aβ) and tau pathologies. This study aims to evaluate the relationships between microstructural white matter injury, cognitive decline and AD core biomarkers.

Methods: We conducted a longitudinal study of 566 participants using peak width of skeletonized mean diffusivity (PSMD) to quantify microstructural white matter injury. The associations of PSMD with changes in cognitive functions, AD pathologies (Aβ, tau, and neurodegeneration), and volumes of AD-signature regions of interest (ROI) or hippocampus were estimated. The associations between PSMD and the incidences of clinical progression were also tested. Covariates included age, sex, education, *apolipoprotein E4* status, smoking, and hypertension.

Results: Higher PSMD was associated with greater cognitive decline (β=-0.012, $P < 0.001$ for Mini-Mental State Examination score; β<0, $P < 0.05$ for four cognitive domains) and a higher risk of clinical progression from normal cognition to mild cognitive impairment (MCI) or AD (Hazard ratio=2.11 [1.38–3.23], $P < 0.001$). These associations persisted independently of amyloid status. PSMD did not predict changes in Aβ or tau levels, but predicted changes in volumes of AD-signature ROI (β=-0.003, $P < 0.001$) or hippocampus (β=-0.002, $P = 0.010$). Besides, the whole-brain PSMD could predict cognitive decline better than regional PSMDs.

Conclusions: PSMD may be a valuable biomarker for predicting cognitive decline and clinical progression to MCI and AD, providing insights besides traditional Aβ and tau pathways. Further research could elucidate its role in clinical assessments and therapeutic strategies.

1. Introduction

With the global population aging, cognitive impairment has become a significant public health challenge [1]. The gradual decline in cognitive abilities not only impairs individuals' quality of life but also imposes a substantial burden on healthcare systems worldwide. Understanding the complex mechanisms behind cognitive decline is crucial. In addition to the well-known effects of amyloid-beta (Aβ) and tau pathology on cognition, damage to brain microstructure also plays an important role [2]. The peak width of skeletonized mean diffusivity (PSMD), a parameter based on diffusion tensor imaging (DTI), can assess microstructural white matter damage [3,4]. White matter, composed of myelinated nerve fibers, facilitates communication between different brain regions and plays a crucial role in cognitive processing. Changes in white matter integrity measured by PSMD have been found to be associated with various neurological disorders, like Alzheimer's disease (AD), cerebral amyloid angiopathy (CAA) and multiple sclerosis [5–7].

Previous studies have identified a significant association between PSMD and cognitive function, particularly in cohorts with CAA [5,8,9]. However, research exploring the relationship between PSMD and cognitive progression in the elderly population remains rare. Specifically, the relationship between PSMD and established core

* Corresponding author at: Department of Neurology, Huashan Hospital, Fudan University, No. 12 Wulumuqi Road, Shanghai, PR China; Department of Neurology, Qingdao Municipal Hospital, Qingdao University, No.5 Donghai Middle Road, Qingdao, PR China.
E-mail addresses: 530852713@qq.com (H.-Y. Hu), hqli12@fudan.edu.cn (H.-Q. Li), weikang.gong@ndcn.ox.ac.uk (W.-K. Gong), hhuang_hsy@163.com (S.-Y. Huang), yanfu_a@163.com (Y. Fu), qingdaoshennei@163.com (H. Hu), dong_qiang@fudan.edu.cn (Q. Dong), wcheng@fudan.edu.cn (W. Cheng), dr.tanlan@163.com (L. Tan), cuimei@fudan.edu.cn (M. Cui), jintai_yu@fudan.edu.cn (J.-T. Yu).
[1] The authors contributed equally to the present work.

https://doi.org/10.1016/j.tjpad.2024.100037
Received 28 October 2024; Received in revised form 9 December 2024; Accepted 10 December 2024
Available online 1 January 2025

AD biomarkers, namely Aβ and tau protein, has not been widely investigated.

Our research aims to elucidate the relationship between microstructural white matter injury, cognitive decline and core AD biomarkers through a longitudinal study. Additionally, we seek to determine whether the relationship between brain microstructural damage and cognitive decline is dependent on the presence of amyloid and tau pathology. Furthermore, our study will, for the first time, delve into the topography of brain region-level PSMD and its association with cognition and clinical outcomes. Through this multifaceted research approach, we aim to reveal the role of microstructural white matter injury in cognitive decline, thereby providing new avenues for the diagnosis and management strategies of cognitive disorders.

2. Methods

2.1. Data source and study population

The Alzheimer's Disease Neuroimaging Initiative (ADNI) database (http://adni.loni.usc.edu/) was the source of data for the main analysis. Detailed inclusion and exclusion criteria for ADNI have been published previously [10]. Diagnosis of AD were based on the National Institute of Neurological and Communication Disorders/Alzheimer's Disease and Related Disorders Association criteria, requiring patients to have a Mini-Mental State Examination (MMSE) score between 20 and 26, a global Clinical Dementia Rating (CDR) from 0.5 to 1.0, and a sum-of-boxes CDR (CDR-SB) score of 1.0–9.0. Patients with mild cognitive impairment (MCI) were characterized by an MMSE score between 24 and 30, objective memory loss confirmed by the Wechsler Memory Scale Logical Memory II delayed recall, a CDR-SB score of at least 0.5, maintained daily living activities, and no dementia. Cognitively normal (CN) controls had an MMSE score of at least 24 and a CDR-SB score of 0 or 0.5. The ADNI study received approval from the institutional review boards of all participating centers, and all participants provided written informed consent. Only ADNI participants with complete diffusion-weighted imaging (DWI) data were included in this study.

2.2. PSMD calculation

We referred to the processing procedures and parameters from previous literature, using the MRtrix v3.0 package (http://mrtrix.org) and the Functional Magnetic Resonance Imaging of the Brain software library (FSL), v6.0.5 [5,11,12]. After preprocessing, PSMD was calculated using the fully automated script (http://www.psmd-marker.com). Finally, using the jhu-icbm-labels-1 mm template (https://neurovault.org/images/1401/), PSMD was calculated for each brain region.

2.3. Magnetic resonance imaging (MRI) measures

High-quality T1-weighted neuroimaging data were used to derive brain structural measures. The 2010 Desikan-Killany atlas guided FreeSurfer in quantifying regional volumes. Volumetric data for the hippocampus and an AD-signature region of interest (ROI), which included the entorhinal, fusiform, inferior temporal, and middle temporal cortices, were utilized [13,14]. Volumetric measures of frontal and parietal lobes were also extracted. Each of the hippocampus, AD-signature ROI, as well as frontal and parietal regions were divided by the intracranial volume (ICV) to eliminate the influence of brain volume.

2.4. PET imaging and CSF biomarkers

We used ADNI pipeline preprocessed positron emission tomography (PET) data for Aβ (florbetapir, or [18F] AV45; florbetaben, or FBB), tau (flortaucipir, or [18F] AV1451), and Fluorodeoxyglucose (FDG). To calculate the mean standard uptake value ratio (SUVR) for each scan, the tracer uptake in the targeted ROI was divided by the value in a predefined reference region according to the protocol (http://adni.loni.usc.edu/datasamples/pet/). ROIs were defined using Freesurfer (version 7.1.1) based on each subject's most recent MRI image for segmentation. To calculate a composite SUVR for each FDG PET scan, the mean uptake of predefined MetaROIs (including bilateral angular, posterior cingulate, and inferior temporal gyrus) was used relative to the mean uptake in a pons/vermis reference region [15]. For Aβ PET, the SUVRs were generated by averaging the uptake ratios across summarized cortical regions associated with AD (frontal, anterior/posterior cingulate, lateral parietal, and lateral temporal regions). These were then normalized using a composite reference region, which included the whole cerebellum, brainstem/pons, and eroded subcortical white matter. When compared with using solely cerebellum as a reference, this composite reference region yielded more reliable longitudinal AV45 results in ADNI [16,17]. To compute a composite SUVR for tau PET, the AV1451 uptake in a weighted composite (MetaROI) of regions, including the bilateral entorhinal, amygdala, fusiform, and inferior and middle temporal cortices, was referenced against the mean uptake of the gray matter in the inferior cerebellum [18,19]. The tau PET SUVR values were extracted from Braak stage ROIs, encompassing three Braak region groups (Braak I, Braak III-IV, and Braak V-VI) in the current study. However, the Braak II region (hippocampus) was excluded due to known off-target binding contamination in the choroid plexus. Additionally, cortical uptake of AV45 and AV1451 in 68 ROIs, as defined by the Desikan-Killiany atlas, was extracted from each PET scan co-registered with the corresponding individual structural MRI scan. The cutoffs for brain Aβ, tau, and FDG PET categories were established as follows: 0.78 for AV45 SUVR, 0.74 for FBB SUVR, 1.37 for AV1451 MetaROI SUVR [19], and 1.21 for FDG PET [15,20].

Cerebrospinal fluid (CSF) was collected by lumbar puncture from a subset of ADNI participants. The specific methods for CSF collection, storage, and measurement were as previously described [21]. The cutoff values for CSF Aβ42, p-tau181, and t-tau were set based on previous literature at 1098 pg/ml [22], 26.64 pg/ml [19], and 300 pg/ml [23], respectively.

The amyloid (A) status of participants was defined based on the abnormal status of CSF Aβ42 as well as amyloid PET (AV45 and FBB). If any one of the three biomarkers indicated an abnormal level of amyloid pathology, the individual would be considered as A positive status.

2.5. Cognitive assessments

We used the MMSE score to represent global cognitive function. Specific cognitive domains were evaluated using the episodic memory (MEM) score, executive function (EF) composite score, and the recently validated language (LAN) and visual-spatial (VS) function score. The MEM score measured the ability to recall specific events and experiences from one's past. The EF composite score assessed higher-level cognitive processes, like problem-solving, planning, and attention. The LAN score evaluated verbal abilities, including comprehension and expression. The VS function score measured the capacity to understand and manipulate visual and spatial information.

2.6. Statistical analysis

The characteristics of participants were described using mean ± standard deviation (SD) for normally distributed data, median and interquartile range (IQR) for non-normally distributed data, and frequency (percentage) for categorical variables. At baseline (first DTI measurement), participants were categorized into CN, MCI, and AD groups. Comparisons among groups were conducted using one-way ANOVA, chi-square tests, or Kruskal-Wallis tests.

Multiple linear regression models were performed to examine the associations between baseline PSMD (whole-brain PSMD and PSMD of 48 individual brain regions) and baseline AD phenotypes, with PSMD as the

independent variables and AD phenotypes as the dependent variables. The AD phenotypes included cognitive functions (MMSE, MEM, EF, LAN and VS scores), MRI measures (AD-signature ROI volume/ICV and hippocampal volume/ICV), CSF AD core biomarkers (Aβ42, p-tau181, t-tau, and p-tau/Aβ42, t-tau/Aβ42), and PET imaging (amyloid: AV45, FBB; tau: AV1451; neurodegeneration: FDG). Variables were log10-transformed to ensure normality. Model 1 was adjusted for age at baseline; model 2 was additionally adjusted for sex, education, *apolipoprotein E4 (APOE4)* status, smoking, and hypertension history. Bonferroni correction was applied for the analyses of PSMD in multiple brain regions, with statistical significance set at $P < 0.001041667$ (0.05 divided by 48 tests).

Subsequently, linear mixed-effects models (LMEMs) were utilized to investigate whether baseline PSMD could predict longitudinal changes in cognitive functions, MRI measures, CSF AD core biomarkers, and PET imaging. The LMEMs regarded the interaction between time and PSMD as predictors. In addition, the LMEMs included random intercepts and slopes for time, as well as an unstructured covariance matrix for random effects. The random effects in LMEMs represented the randomness and variability in different individuals. Moreover, the annual rates of change in these AD phenotypes were calculated using LMEMs, and then the associations between PSMD and the rates of change in these AD phenotypes were analyzed. Model 1 was adjusted for age at baseline; model 2 was additionally adjusted for sex, education, *APOE4* status, smoking, and hypertension. To maximize the use of data for longitudinal analyses, for participants who did not have a CSF, MRI or cognitive assessment at baseline (first DTI measurement), their corresponding measurements within one-year following baseline PSMD measurement were used for imputation.

Cox proportional hazard regression models were conducted to examine the associations between baseline PSMD and the risks of clinical progressions, with the duration of follow-up as the timescale. PSMD values were used as both continuous and categorical variables (low [reference], median, high tertiles). The clinical progressions included the conversion from CN to MCI, conversion from CN to AD, as well as conversion from MCI to AD. Analyses restricted in CN participants were repeated, in which the clinical progression was defined as conversion from CN to MCI or AD. Follow-up began from DTI baseline to the date of the earliest clinical progression, or the last recorded time. Model 1 was adjusted for age at baseline; model 2 was additionally adjusted for sex, education, *APOE4* status, smoking, and hypertension. Hazard ratios (HRs) with 95% confidence intervals (CIs) were reported.

To further explore the longitudinal association of PSMD with AD core pathology, Cox regression models were also conducted to test whether baseline PSMD could predict amyloid status progression (conversion from A- to A+) after adjusting for age. Follow-up began from DTI baseline to the date of the earliest conversion to A+, or the last recorded time. Analyses were conducted in the total participants as well as restricted in CN participants, respectively.

Furthermore, we performed two additional analyses. First, to test whether PSMD exacerbated neurodegeneration only through AD-related neuronal injury or if also through other non-AD pathologies, the associations between PSMD and frontal or parietal lobes, which were not included in AD-signature ROI, were examined. Second, subgroup analyses stratified by baseline amyloid status were performed to test whether PSMD contributed to cognitive decline or MRI volumetric changes in the A- participants, who were presumed to be non-AD.

R version 4.1.2 and GraphPad Prism 8.0.2 software were used for statistical analyses and figure preparation. A P value <0.05 was considered significant, except where specifically noted.

3. Results

3.1. Participant characteristics

Baseline characteristics of the subjects were summarized in Table 1. We included a total of 566 subjects with an average age of 68.23 years (SD=4.64), of which 314 (55.5%) were female. The baseline popula-

Table 1
Characteristics of the study population.

	Total (N = 566)	CN (N = 310)	MCI (N = 187)	AD dementia (N = 60)	P value
Age (years, mean [SD])	68.23 (4.64)	68.25 (4.11)	68.34 (5.18)	68.06 (5.47)	0.918*
Sex (female,%)	314 (55.5)	194 (62.6)	81 (43.3)	32 (53.3)	<0.001†
Education (years, median [IQR])	16 (15, 18)	17 (16, 18)	16 (14, 18)	16 (13, 18)	<0.001§
APOE4 status (%)					<0.001†
ε4-/-	256 (52.0)	170 (62.7)	72 (45.0)	10 (17.5)	
ε4-/+	191 (38.8)	95 (35.1)	62 (38.8)	34 (59.6)	
ε4+/+	45 (9.1)	6 (2.2)	26 (16.2)	13 (22.8)	
Smoking (yes,%)	127 (22.4)	65 (21.0)	47 (25.1)	14 (23.3)	0.555†
Hypertension (yes,%)	228 (40.3)	110 (35.5)	88 (47.1)	25 (41.7)	0.037†
PSMD (mean [SD])	8.85E-04 (1.87E-04)	8.43E-04 (1.65E-04)	9.01E-04 (1.77E-04)	1.06E-03 (2.18E-04)	<0.001*
MMSE Score (mean [SD])	28.04 (2.75)	29.19 (0.98)	27.92 (1.90)	22.37 (4.00)	<0.001*
ADNI_MEM (mean [SD])	0.68 (0.92)	1.17 (0.58)	0.35 (0.67)	−0.92 (0.72)	<0.001*
ADNI_EF (mean [SD])	0.74 (1.06)	1.15 (0.81)	0.54 (0.84)	−0.82 (1.22)	<0.001*
ADNI_LAN (mean [SD])	0.60 (0.92)	0.96 (0.75)	0.37 (0.73)	−0.56 (1.04)	<0.001*
ADNI_VS (mean [SD])	0.05 (0.81)	0.24 (0.64)	0.01 (0.76)	−0.81 (1.15)	<0.001*
CSF Aβ_{42} (pg/ml, mean [SD])	1110.60 (619.60)	1274.54 (624.19)	1081.42 (592.45)	613.27 (321.96)	<0.001*
CSF p-tau181 (pg/ml, mean [SD])	24.37 (14.10)	20.15 (8.44)	26.01 (16.77)	36.01 (16.57)	<0.001*
CSF t-tau (pg/ml, mean [SD])	259.07 (123.98)	224.45 (82.65)	269.84 (138.96)	362.20 (152.19)	<0.001*
AV45 PET SUVR (mean [SD])	1.17 (0.21)	1.10 (0.14)	1.18 (0.23)	1.44 (0.18)	<0.001*
FBB PET SUVR (mean [SD])	1.14 (0.22)	1.10 (0.16)	1.13 (0.21)	1.44 (0.32)	<0.001*
AV1451 PET SUVR (mean [SD])	1.27 (0.28)	1.18 (0.12)	1.32 (0.30)	1.73 (0.49)	<0.001*
FDG PET SUVR (mean [SD])	1.22 (0.17)	1.32 (0.13)	1.25 (0.13)	1.00 (0.16)	<0.001*
Amyloid status (amyloid positivity,%)	190 (42.2)	82 (33.6)	67 (44.6)	40 (74.0)	<0.001†
Residual hippocampal volume (cm3, mean [SD])	7406.32 (1078.89)	7746.56 (811.99)	7324.51 (1052.24)	5858.88 (1062.71)	<0.001*
Residual AD-signature ROI volume (cm3, mean [SD])	64,167.05 (8526.04)	65,647.32 (7466.26)	64,824.13 (8084.52)	54,857.70 (9303.07)	<0.001*

NOTE: Data were compared using one-way ANOVA*, chi-square tests† or Kruskal-Wallis tests§.
Abbreviations: CN, cognitively normal; MCI, mild cognitive impairment; AD, Alzheimer's disease; SD, standard deviations; IQR, interquartile range; *APOE4, apolipoprotein E4*; PSMD, peak width of skeletonized mean diffusivity; MMSE, Mini-Mental State Examination; ADNI, Alzheimer's Disease Neuroimaging Initiative; MEM, memory composite score; EF, executive function composite score; LAN, language composite score; VS, visuospatial function composite score; CSF, cerebrospinal fluid; Aβ, β-amyloid; p-tau181, phosphorylated tau 181; t-tau, total tau; AV45, florbetapir; PET, positron emission tomography; SUVR, standard uptake value ratio; FBB, florbetaben; AV1451, flortaucipir; FDG, fluorodeoxyglucose; ROI, region of interest.

tion with normal cognition consisted of 310 individuals (54.5%). During a median follow-up period of 3.16 years (IQR=2.04–4.19), a total of 59 (16.2%) non-dementia individuals experienced clinical progression, transitioning to MCI or AD.

3.2. PSMD and cognitive functions

Fig. 1 illustrated the cross-sectional associations between baseline PSMD and cognitive scores (including MMSE, ADNI-MEM, ADNI-EF, ADNI-LAN, and ADNI-VS). Baseline whole-brain PSMD values were negatively correlated with cognitive scores (model 1; MMSE, β=−0.167, P = 4.12E-11; ADNI_MEM, β=−3.105, P = 1.72E-12; ADNI_EF, β=−3.679, P = 2.93E-13; ADNI_LAN, β=−2.361, P = 9.98E-08; ADNI_VS, β=−1.858, P = 1.99E-06; Fig. 1A). The results were stable in model 2 (Supplementary Table 1). Fig. 1B demonstrated the relationships between PSMD values of different brain regions and cognitive scores. Significant negative correlations were observed between cognitive scores and PSMD values across multiple white matter tracts (model 1, P<Bonferroni correction threshold; Supplementary Table 2). However, the correlations between PSMD values of individual brain regions and cognitive function were not as significant as those between whole-brain PSMD and cognitive function. The results of brain regions were stable in model 2 (Supplementary Table 3).

3.3. PSMD predicted cognitive decline and the clinical progressions

Description of longitudinal data in the current study was shown in Supplementary Table 4. The results of LMEMs for MMSE score and the four cognitive domains were summarized in Table 2. Baseline PSMD could predict the longitudinal cognitive decline (model 1; MMSE, β=−0.012, P = 5.05E-06; ADNI_MEM, β=−0.055, P = 2.29E-07; ADNI_EF, β=−0.027, P = 0.003; ADNI_LAN, β=−0.058, P = 1.67E-06; ADNI_VS, β=−0.029, P = 0.012). The results were stable in model 2. Meanwhile, the greater baseline PSMD was associated with faster annual rates of decline in MMSE and cognitive domains scores (P < 0.001 for all; Fig. 2A–E and Supplementary Table 5).

Results of the Cox regression models for predicting clinical progression were shown in Supplementary Table 6. In the entire cohort, 59 individuals experienced clinical progression (including 26 individuals progressing from CN to MCI, 28 individuals progressing from MCI to AD dementia, and 5 individuals progressing from CN to AD dementia). The clinical progression was defined in two ways. The first definition included all clinical conversions: from CN to MCI, from MCI to dementia, and from CN to dementia. The higher PSMD z-score at baseline was significantly associated with an increased risk of clinical progression (model 1, HR [95% CI]=1.516 [1.132–2.030], P = 0.005). When classifying baseline PSMD into tertiles, participants in the high PSMD group

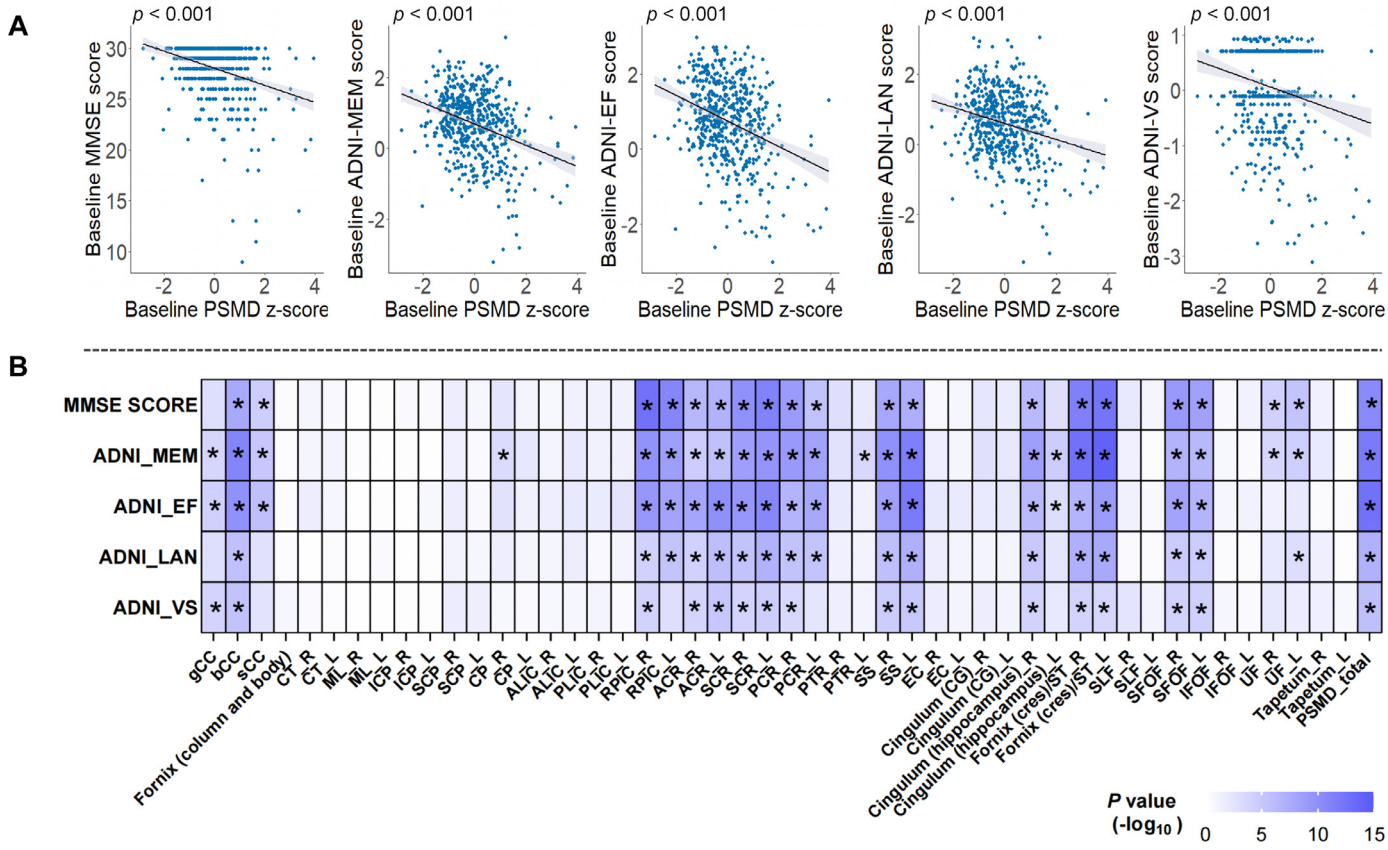

Fig. 1. Cross-sectional associations between PSMD and cognitive functions. The associations of baseline whole-brain PSMD (A) or regional PSMDs (B) with baseline cognitive functions were tested by multiple linear regressions after adjusting for age. Bonferroni correction was applied for the analysis of PSMD in brain regions, with statistical significance set at P < 0.001041667 (0.05 divided by 48 tests).
Abbreviations: PSMD, peak width of skeletonized mean diffusivity; MMSE, Mini-Mental State Examination; ADNI, Alzheimer's Disease Neuroimaging Initiative; MEM, memory composite score; EF, executive function composite score; LAN, language composite score; VS, visuospatial function composite score; gCC, genu of corpus callosum; bCC, body of corpus callosum; sCC, splenium of corpus callosum; CT, corticospinal tract; ML, medial lemniscus; ICP, inferior cerebellar peduncle; SCP, superior cerebellar peduncle; CP, cerebral peduncle, ALIC, anterior limb of internal capsule; PLIC, posterior limb of internal capsule; RPIC, retrolenticular part of internal capsule; ACR, anterior corona radiata; SCR, superior corona radiata; PCR, posterior corona radiata; PTR, posterior thalamic radiation; SS, sagittal stratum; EC, external capsule; CG, cingulate gyrus; ST, stria terminalis; SLF, superior longitudinal fasciculus; SFOF, superior fronto-occipital fasciculus; IFOF, inferior fronto-occipital fasciculus; UF, uncinate fasciculus; R, right hemisphere; L, left hemisphere.

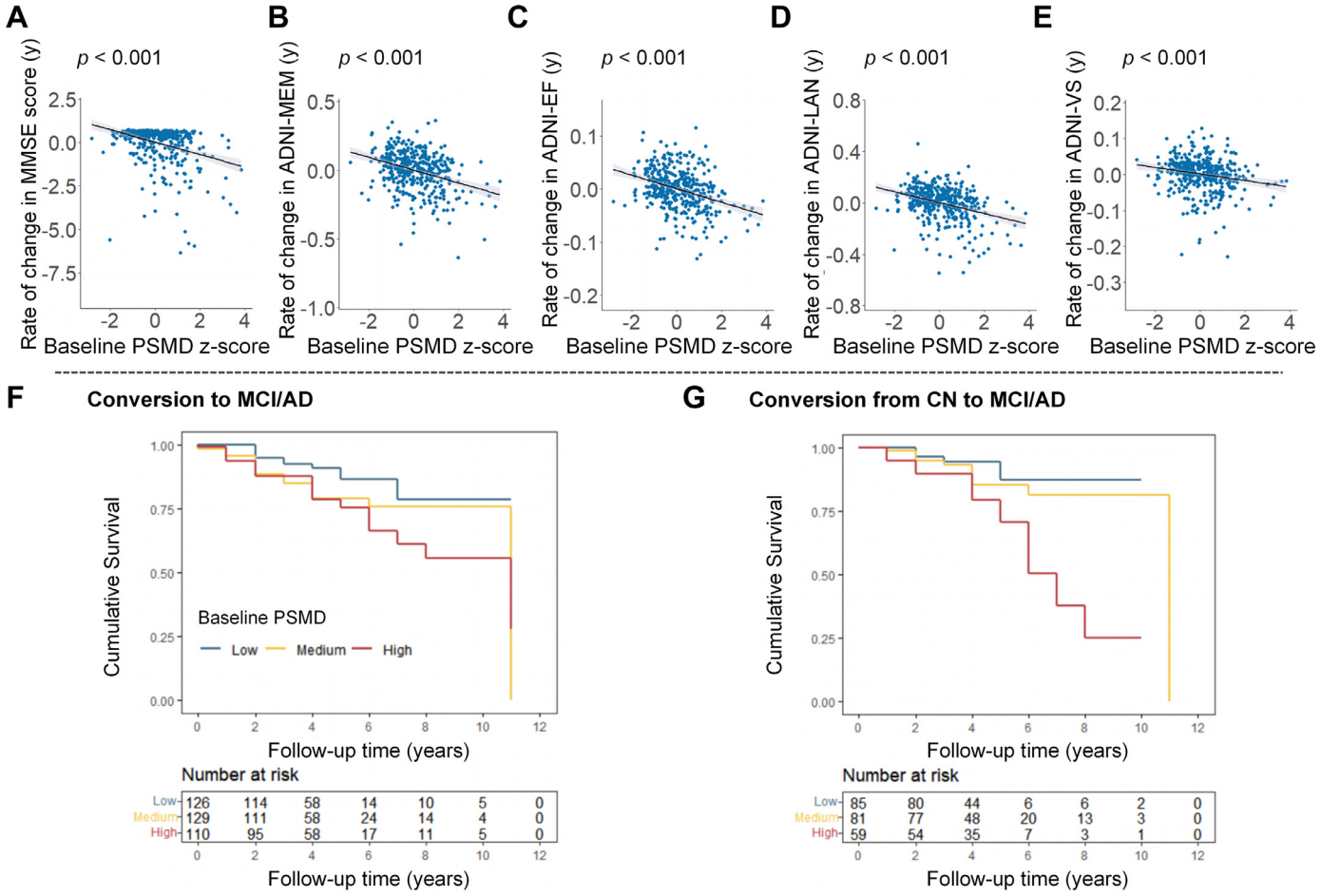

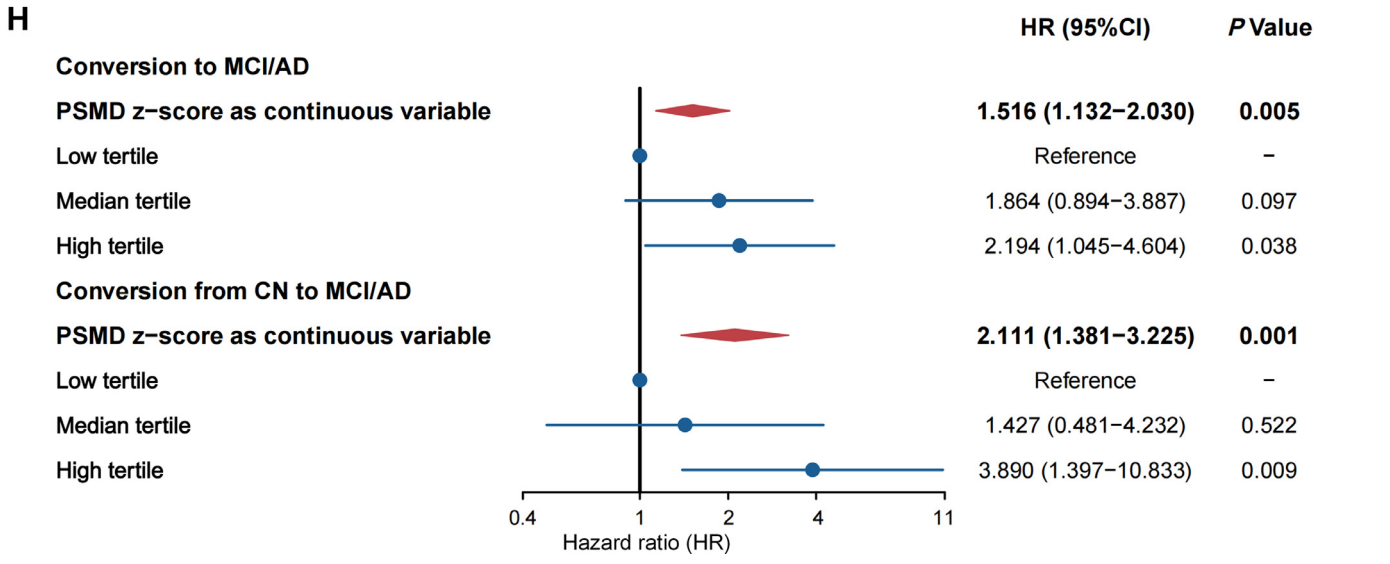

Fig. 2. PSMD predicted clinical progression and cognitive decline. Rates of change in cognitive functions (year) were calculated by mixed linear models after adjusting for age. Then, the associations between baseline PSMD and rates of change in cognitive functions were tested by linear regressions (A-E). Associations between baseline PSMD and the incidences of clinical progression were tested using Cox proportional hazard regression models after adjusting for age (F-H).
Abbreviations: PSMD, peak width of skeletonized mean diffusivity; MMSE, Mini-Mental State Examination; ADNI, Alzheimer's Disease Neuroimaging Initiative; MEM, memory composite score; EF, executive function composite score; LAN, language composite score; VS, visuospatial function composite score; MCI, mild cognitive impairment; AD, Alzheimer's disease; CN, cognitively normal; HR, hazard ratios; CI, confidence intervals.

Table 2
Prediction of changes in cognitive function or AD biomarkers by baseline PSMD z-score.

Variables	Model 1		Model 2	
	Beta	*P* value	Beta	*P* value
Cognitive function				
MMSE Score	−0.012	**5.05E-06**	−0.012	**3.44E-05**
ADNI_MEM	−0.055	**2.29E-07**	−0.052	**1.71E-06**
ADNI_EF	−0.027	**0.003**	−0.024	**0.009**
ADNI_LAN	−0.058	**1.67E-06**	−0.055	**8.24E-06**
ADNI_VS	−0.029	**0.012**	−0.026	**0.024**
MRI measures				
AD-signature ROI volume / ICV	−0.003	**4.38E-05**	−0.002	**1.03E-04**
Hippocampal volume / ICV	−0.002	**0.010**	−0.002	**0.012**
CSF measures				
CSF Aβ42	0.005	0.218	0.005	0.216
CSF p-tau181	−0.002	0.353	−0.002	0.342
CSF t-tau	−7.52E-04	0.701	−8.13E-04	0.677
CSF p-tau/Aβ42	−0.007	0.114	−0.008	0.097
CSF t-tau/Aβ42	−0.007	0.119	−0.007	0.116
PET biomarkers				
AV45 PET SUVR	1.42E-04	0.769	2.94E-05	0.952
FBB PET SUVR	6.40E-04	0.429	5.69E-04	0.487
AV1451 PET SUVR	9.38E-04	0.311	4.75E-04	0.598
FDG PET SUVR	−0.002	0.193	−0.002	0.229

NOTE: Each of the AD ROI and hippocampus were divided by the ICV to eliminate the influence of brain volume.
Associations between baseline PSMD and longitudinal data (cognitive functions, MRI measures, CSF AD core biomarkers, PET biomarkers) were tested by mixed linear models. Model 1 was adjusted for age. Model 2 was adjusted for age, sex, education, *APOE4* status, smoking and hypertension history.
Abbreviations: AD, Alzheimer's disease; PSMD, peak width of skeletonized mean diffusivity; MMSE, Mini-Mental State Examination; ADNI, Alzheimer's Disease Neuroimaging Initiative; MEM, memory composite score; EF, executive function composite score; LAN, language composite score; VS, visuospatial function composite score; MRI, magnetic resonance imaging; ROI, region of interest; ICV, intracranial volume; CSF, cerebrospinal fluid; Aβ, β-amyloid; p-tau181, phosphorylated tau 181; t-tau, total tau; PET, positron emission tomography; AV45, florbetapir; SUVR, standard uptake value ratio; FBB, florbetaben; AV1451, flortaucipir; FDG, fluorodeoxyglucose; *APOE4, apolipoprotein E4*.

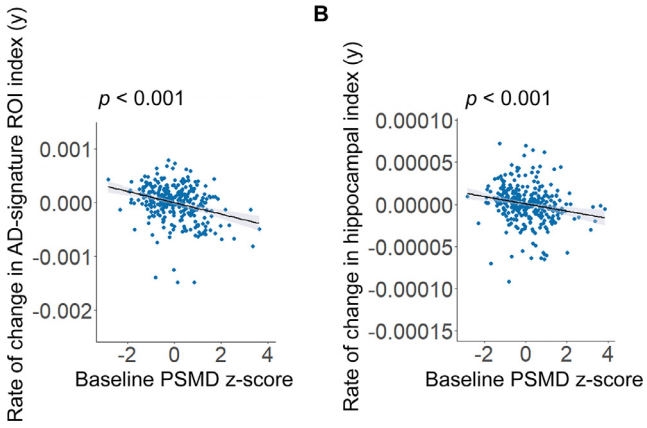

Fig. 3. Associations between baseline PSMD and rates of changes in AD-signature ROI or hippocampal volumes. Each of the AD ROI (A) and hippocampus (B) were divided by the ICV to eliminate the influence of brain volume. Rates of change in MRI measures (year) were calculated by mixed linear models after adjusting for age. Then, the associations between baseline PSMD and rates of change in MRI measures were tested by linear regressions.
Abbreviations: PSMD, peak width of skeletonized mean diffusivity; AD, Alzheimer's disease; ROI, region of interest; ICV, intracranial volume; MRI, magnetic resonance imaging.

were 2.19 times more likely to experience clinical progression (model 1, HR [95% CI]=2.194 [1.045–4.604], P = 0.038; Fig. 2F and 2H). The above results were stable in model 2.

The second definition of clinical progression included only those who progressed from being CN at baseline to MCI or AD. The higher PSMD z-score at baseline was associated with an increased risk of clinical progression (model 1, HR [95% CI]=2.111[1.381–3.225], P < 0.001). In reference to the low PSMD group, participants in the high group showed a significantly higher risk of progression to MCI or AD dementia in both the unadjusted KM curves and multivariable Cox regression models (model 1, HR [95% CI]=3.890 [1.397–10.833], P = 0.009; Fig. 2G and H). The results were stable in model 2.

3.4. PSMD and AD biomarkers

The cross-sectional associations between whole-brain PSMD and AD biomarkers were summarized in Supplementary Table 1. Baseline whole-brain PSMD was significantly associated with baseline CSF Aβ42 (model 1, β=−0.732, P = 1.18E-06), AD-signature ROI volume (β=−0.153, P = 1.24E-09), hippocampal volume (β=−0.337, P = 1.08E-24), and FDG PET SUR (β=−0.420, P = 3.14E-19), but the associations for CSF p-tau181 and t-tau did not reach a Bonferroni-corrected significance. The results were stable in model 2. For individual brain regions, significant associations were still observed between PSMD values across multiple tracts and CSF Aβ42, AD-signature ROI volume, hippocampal volume, and FDG PET SUR (model 1, P<Bonferroni correction threshold; Supplementary Tables 7–9), but not with CSF p-tau181 or t-tau. The pattern of correlations between PSMD values of individual brain region and AD biomarkers was similar to that between PSMD and cognitive function. These findings suggested that the association between PSMD values and cognitive impairment might be due to damage in key cognitive brain regions. The above results of brain regions were stable in model 2 (Supplementary Tables 10–12). Supplementary Fig. 1 summarized the cross-sectional associations between PSMD in brain regions and AD biomarkers.

The results of LMEMs were shown in Table 2. Baseline PSMD could predict longitudinal changes in AD-signature ROI (model 1, β=−0.003, P = 4.38E-05) and hippocampal volumes (β=−0.002, P = 0.010). The results were stable in model 2. Meanwhile, a greater baseline PSMD was associated with a faster annual rate of decline in AD-signature ROI (β=−1.05E-04, P = 2.01E-08) or hippocampal volume (β=−4.38E-06, P = 6.59E-04; Fig. 3 and Supplementary Table 13). With regards to the longitudinal relationships between PSMD and amyloid or tau pathologies, however, we found that baseline PSMD could not predict changes in CSF AD core biomarkers (models 1–2, P > 0.05 for all CSF biomarkers; Table 2). Nor did baseline PSMD predict changes in Aβ PET, AV1451 PET and FDG PET SUVRs (models 1–2, P > 0.05 for all PET biomarkers; Table 2). Moreover, the results of COX regression models showed that baseline PSMD could not predict the amyloid-positive conversion (P > 0.05; Supplementary Table 14).

3.5. Additional analyses

Significant cross-sectional associations of PSMD with frontal- and parietal- regional volumes were found (Supplementary Table 15). The LMEMs showed that baseline PSMD could predict the longitudinal changes in caudal-middle-frontal, rostral-middle-frontal and lateral-orbito-frontal volumes, as well as change in superior-parietal volume (Supplementary Table 16).

Moreover, the subgroup analyses showed that baseline PSMD was negatively associated with baseline cognitive functions, AD-signature ROI volume and hippocampal volume in both of the A- and A+ groups (Supplementary Table 17). PSMD could accelerate longitudinal cognitive decline in both A- and A+ groups (Supplementary Table 18). As for MRI measures, the longitudinal correlations between PSMD and AD-signature ROI or hippocampal volumetric changes were more significant

in A+ than in A- group (Supplementary Table 18). These findings suggested that PSMD could exacerbate neurodegeneration, which has no AD-specificity and was applicable to non-AD pathology.

4. Discussion

This study investigated the predictive capability of the PSMD as a biomarker for cognitive decline. Our results indicated a significant correlation between PSMD and cognitive decline, with whole brain PSMD values being significantly higher in the cognitive decline group compared to the cognitively stable group. Also, it is noteworthy that PSMD could predict longitudinal changes in AD-signature ROIs and hippocampal volumes. Our study also found a close relationship between specific white matter tracts and AD-signature ROIs. For example, the anterior limb of the internal capsule (ALIC), posterior limb of the internal capsule (PLIC), the retrolenticular part of internal capsule (RPIC), and cingulum all showed a significant negative correlation with AD-signature ROIs. Besides, there was no correlation between PSMD and the progression of AD core biomarkers. These findings suggested that PSMD could serve as an independent biomarker besides Aβ and tau pathology, aiding in identifying individuals at risk of cognitive decline. Larger longitudinal studies are needed in the future to further elucidate the causal relationship between PSMD and cognitive decline.

Our results aligned with previous hypotheses that white matter integrity played a crucial role in cognitive function [24]. Previous literature has extensively reported the correlation between PSMD and cognitive decline, primarily focusing on patients with cerebrovascular diseases, including cerebral autosomal dominant arteriopathy with subcortical infarcts and leukoencephalopathy (CADASIL) [4], sporadic cerebral small vessel disease (SVD) [4], and CAA [5,25,26]. PSMD was significantly associated with overall cognitive decline and a decrease in processing speed [4,25]. Additionally, in population cohorts such as Chinese university of Hong Kong–risk index for subclinical brain lesions in Hong Kong (CU-RISK) cohort, neuroinflammation in memory and related other disorders (NIMROD) cohort, and Hamburg city health study (HCHS) cohort, a correlation has been found between PSMD and the decline in global cognitive status, processing speed, and EF [27–29]. The correlation between PSMD and cognitive decline was consistent with existing literature, indicating that abnormalities in white matter microstructure were a significant factor contributing to cognitive impairment. A large body of previous research using DTI has explored the microstructural changes in the brain white matter of AD patients [30–32]. In AD patients, due to neurodegeneration, particularly neuronal degradation and demyelination, the directionality of water molecule diffusion was disrupted, resulting in a significant decrease in fractional anisotropy (FA) and an increase in mean diffusivity (MD) [33,34]. These changes reflected microstructural damage to white matter and were closely associated with cognitive impairment in AD. However, few previous studies have simultaneously investigated the relationship between PSMD, cognition, and AD core biomarkers. Our study extended previous research by demonstrating the predictive capability of PSMD independent of traditional Aβ and tau biomarkers. Microstructural white matter damage played a vital role in cognitive decline, and PSMD, as an indicator of this damage, had significant advantages. Compared to traditional structural MRI markers, such as the mean FA and other established MD metrics, PSMD had higher specificity and could more accurately reflect changes in white matter microstructure [28,35]. Additionally, PSMD measurement methods were simple and highly reproducible, making it a potential clinical biomarker.

Furthermore, our research has identified a close correlation between the patterns of white matter tract damage and declines in cognitive function scores, particularly in memory, executive function, language abilities, and visuospatial skills. Significant correlations existed between the PSMD values of the corpus callosum tracts (genu of corpus callosum [gCC], body of corpus callosum [bCC], splenium of corpus callosum [sCC]) and cognitive scores in memory and executive function, with the bCC showing the strongest correlation. Damage to the corpus callosum influenced the communication between the left and right cerebral hemispheres, potentially leading to trans-hemispheric information transfer disorders and further cognitive decline [36,37]. Damage to subcortical pathways such as the RPIC, anterior corona radiata (ACR), superior corona radiata (SCR) and uncinate fasciculus (UF) were also closely linked to multidimensional cognitive impairments. These pathways played crucial roles in motor control and sensory processing, and their damage could lead to a comprehensive decline in cognitive functions [38]. Damage in the hippocampus and limbic systems, such as the cingulum, was also strongly correlated with increases in PSMD values. These areas were intimately associated with memory, emotion, and learning functions. Hippocampal damage was significantly related to declines in episodic memory, supporting the critical role of these areas in early cognitive decline [30]. Differences in PSMD values and cognitive function scores between the left and right hemispheres might reflect the distinct roles of each hemisphere in specific cognitive tasks, such as in executive functions and language abilities. Previous studies have indicated widespread diffusion measure abnormalities in association fibers such as the corpus callosum, corona radiata and hippocampus in AD patients [39]. Our findings were consistent with these patterns, underscoring the robustness of this study.

In previous histopathological and imaging correlation studies involving CAA and MS populations, DTI metric MD has been found to be closely associated with myelin density, axonal count, and tissue rarefaction [40,41]. Therefore, we had reason to infer that the association between PSMD and cognitive decline might be attributed to white matter damage caused by disruptions in neural connectivity and information processing. Furthermore, inflammatory responses associated with white matter damage might exacerbate neurodegeneration, further leading to cognitive decline [42]. Abnormalities in white matter microstructure could impair neural networks, affecting information transmission and integration, thereby impacting cognitive function. However, there is currently a lack of clinical or basic research elucidating the biological mechanisms underlying the association between PSMD and cognitive decline. Future research should explore the relationship between PSMD and biological processes such as neuronal damage and inflammatory responses to comprehensively understand its role in cognitive decline. Our findings highlighted the importance of considering white matter integrity in understanding cognitive deterioration.

Although PSMD did not predict longitudinal changes in CSF AD core biomarkers, PSMD showed significant association with CSF AD core biomarkers at baseline. We proposed that CSF AD core biomarkers might have reached a plateau early in the disease process, which could explain the lack of significant longitudinal changes [43,44]. Aβ deposition and tau pathology typically occurred before the onset of clinical symptoms and might rapidly reach a saturation point early in the disease. Once the clinical stage was reached, the concentrations of Aβ and tau in CSF might plateau, reducing their predictive ability for cognitive progression in longitudinal analyses. This could explain why, despite a baseline association, CSF AD core biomarkers are not reliable predictors of cognitive decline over time. In contrast, PSMD, as an imaging marker, might offer more dynamic insights into cognitive progression, while the changes in CSF AD biomarkers might become less informative after reaching a plateau prior to clinical manifestation.

The relationship between white matter hyperintensities (WMH) and AD has been a complex and multifaceted issue, involving various pathological mechanisms, including both vascular factors and the neurodegenerative changes intrinsic to AD [45]. In AD patients, the prevalence and severity of WMH were higher, and WMH were closely associated with cognitive impairment, including the onset of AD [46]. Some perspectives suggested that WMH and AD pathology (such as amyloid plaques and tau pathology) might act independently and additively, with WMH potentially lowering the threshold for AD diagnosis and contributing independently to the development of cognitive impairment [47]. Alternatively, some argued that there might be an interac-

tion between WMH and AD pathology, where each lesion exacerbated the other, leading to more severe cognitive deficits [48]. Our study explored the relationship between white matter microstructural damage and cognitive decline, as well as the onset and progression of AD, using PSMD as an indicator. We found that white matter microstructural damage can promote the onset of cognitive impairment. However, given the rapid accumulation of AD CSF core biomarkers, the relationship between white matter microstructural damage and AD pathology warrants further investigation.

Despite our study providing valuable insights into the predictive capability of PSMD as a biomarker for cognitive decline, there were some limitations. First, our study had a relatively small sample size. Future studies with larger sample sizes are needed to establish the temporal relationship between PSMD and cognitive decline. Second, this study merely demonstrated that PSMD could predict cognitive decline in the elderly population, but it did not explore the mechanisms underlying the association between PSMD and cognitive impairment. Further research is needed to investigate how PSMD mediates the process of cognitive impairment. Future research should also replicate these findings in more diverse samples. Additionally, utilizing multimodal imaging data and comprehensive neuropsychological assessments would offer a more comprehensive understanding of the relationship between PSMD and cognitive decline. Moreover, not only baseline PSMD, but also the longitudinal change in PSMD should better be measured in future studies.

This study has theoretical significance for understanding the pathophysiology of cognitive decline and neurodegenerative diseases. By highlighting the role of white matter integrity in cognitive function, this study underscores the importance of considering non-traditional biomarkers in diagnostic and therapeutic strategies. From a practical application perspective, identifying PSMD as a potential biomarker for cognitive decline has significant clinical implications. PSMD may provide clinicians with a non-invasive tool to identify at-risk patients and intervene early to slow disease progression. Early identification of individuals at risk for cognitive decline could facilitate timely interventions and the development of personalized treatment strategies, thereby maintaining cognitive function and improving patient outcomes.

In conclusion, PSMD can predict the clinical progressions from CN to MCI and AD, suggesting that it may serve as a potential biomarker for cognitive decline or AD beyond traditional Aβ and tau pathways. This finding is crucial for early diagnosis and clinical management. In future, the relationship between PSMD and Aβ accumulation still requires further validation through additional clinical and experimental data.

Abbreviations

Aβ, amyloid-beta; PSMD, peak width of skeletonized mean diffusivity; DTI, diffusion tensor imaging; AD, Alzheimer's disease; CAA, cerebral amyloid angiopathy; ADNI, Alzheimer's Disease Neuroimaging Initiative; MMSE, Mini-Mental State Examination; CDR, Clinical Dementia Rating; CDR-SB, sum-of-boxes CDR; MCI, mild cognitive impairment; CN, cognitively normal; DWI, diffusion-weighted imaging; FSL, Functional Magnetic Resonance Imaging of the Brain software library; MRI, magnetic resonance imaging; ROI, region of interest; ICV, intracranial volume; PET, positron emission tomography; AV45, florbetapir; FBB, florbetaben; AV1451, flortaucipir; FDG, fluorodeoxyglucose; SUVR, standard uptake value ratio; CSF, cerebrospinal fluid; MEM, memory; EF, executive function; LAN, language; VS, visual-spatial; SD, standard deviation; IQR, interquartile range; *APOE4, apolipoprotein E4*; LMEM, linear mixed-effects model; HR, hazard ratio; CI, confidence interval; ALIC, anterior limb of the internal capsule; PLIC, posterior limb of the internal capsule; RPIC, retrolenticular part of internal capsule; CADASIL, cerebral autosomal dominant arteriopathy with subcortical infarcts and leukoencephalopathy; SVD, small vessel disease; CU-RISK, Chinese university of Hong Kong–risk index for subclinical brain lesions in Hong Kong; NIMROD, neuroinflammation in memory and related other disorders; HCHS, Hamburg city health study; FA, fractional anisotropy; MD, mean diffusivity; gCC, genu of corpus callosum; bCC, body of corpus callosum; sCC, splenium of corpus callosum; ACR, anterior corona radiata; SCR, superior corona radiata; UF, uncinate fasciculus; WMH, white matter hyperintensities.

Funding

Qiang Dong was supported by grants from the National Key R&D Program of China (2021YFC2500100). Jin-Tai Yu was supported by grants from the STI2030-Major Projects (2022ZD0211600), National Natural Science Foundation of China (82,071,201, 82,271,471, 92,249,305), Project supported by Shanghai Municipal Science and Technology Major Project (2023SHZDZX02), Excellent Academic Research Leader Program of Shanghai (23XD1420400), Emerging Interdisciplinary Research Project of Shanghai (2022JC014), Research Start-up Fund of Huashan Hospital (2022QD002), and ZHANGJIANG LAB, Tianqiao and Chrissy Chen Institute, and the State Key Laboratory of Neurobiology and Frontiers Center for Brain Science of Ministry of Education, Fudan University. The sponsors had no role in the design and conduct of the study; in the collection, analysis, and interpretation of data; in the preparation of the manuscript; or in the review or approval of the manuscript.

Availability of data and materials

The datasets used during the current study are available from the corresponding author on reasonable request.

Consent for publication

Not applicable.

Ethics approval and consent to participate

ADNI was approved by the institutional review boards of all participating centres (https://adni.loni.usc.edu/wp-content/uploads/how_to_apply/ADNI_Acknowledgement_List.pdf), and the written informed consent was obtained from all participants or their authorised representatives according to the Declaration of Helsinki before study enrollment. Ethics approval was obtained from the institutional review boards of each institution involved: Oregon Health and Science University; University of Southern California; University of California—San Diego; University of Michigan; Mayo Clinic, Rochester; Baylor College of Medicine; Columbia University Medical Center; Washington University, St. Louis; University of Alabama at Birmingham; Mount Sinai School of Medicine; Rush University Medical Center; Wien Center; Johns Hopkins University; New York University; Duke University Medical Center; University of Pennsylvania; University of Kentucky; University of Pittsburgh; University of Rochester Medical Center; University of California, Irvine; University of Texas Southwestern Medical School; Emory University; University of Kansas, Medical Center; University of California, Los Angeles; Mayo Clinic, Jacksonville; Indiana University; Yale University School of Medicine; McGill University, Montreal-Jewish General Hospital; Sunnybrook Health Sciences, Ontario; U.B.C. Clinic for AD & Related Disorders; Cognitive Neurology—St. Joseph's, Ontario; Cleveland Clinic Lou Ruvo Center for Brain Health; Northwestern University; Premiere Research Inst (Palm Beach Neurology); Georgetown University Medical Center; Brigham and Women's Hospital; Stanford University; Banner Sun Health Research Institute; Boston University; Howard University; Case Western Reserve University; University of California, Davis—Sacramento; Neurological Care of CNY; Parkwood Hospital; University of Wisconsin; University of California, Irvine—BIC; Banner Alzheimer's Institute; Dent Neurologic Institute; Ohio State University; Albany Medical College; Hartford Hospital, Olin Neuropsychiatry Research Center; Dartmouth-Hitchcock Medical Center; Wake Forest University Health Sciences; Rhode Island Hospital; Butler Hospital; UC San Francisco; Medical University South

Carolina; St. Joseph's Health Care Nathan Kline Institute; University of Iowa College of Medicine; Cornell University and University of South Florida: USF Health Byrd Alzheimer's Institute.

Conflict of Interest

Qiang Dong has received funding from the National Key R&D Program of China (2021YFC2500100). Jin-Tai Yu has received funding from the STI2030-Major Projects (2022ZD0211600), National Natural Science Foundation of China (82,071,201), National Natural Science Foundation of China (82,271,471), National Natural Science Foundation of China (92,249,305), Project supported by Shanghai Municipal Science and Technology Major Project (2023SHZDZX02), nExcellent Academic Research Leader Program of Shanghai (23XD1420400), Emerging Interdisciplinary Research Project ofShanghai (2022JC014), Research Start-up Fund of Huashan Hospital (2022QD002), ZHANGJIANG LAB payments were made to my institutionTianqiao and Chrissy Chen Institute, the State Key Laboratory of Neurobiology and Frontiers Center for Brain Science of Ministry of Education, Fudan University. The other authors do not have any conflict of interest.

CRediT authorship contribution statement

He-Ying Hu: Writing – original draft, Validation, Software, Methodology, Investigation, Formal analysis. **Hong-Qi Li:** Writing – original draft, Validation, Software, Methodology, Formal analysis. **Wei-Kang Gong:** Software, Methodology, Investigation, Formal analysis, Data curation. **Shu-Yi Huang:** Validation, Methodology, Formal analysis. **Yan Fu:** Validation, Methodology. **Hao Hu:** Validation, Formal analysis. **Qiang Dong:** Validation, Funding acquisition. **Wei Cheng:** Data curation. **Lan Tan:** Writing – review & editing, Visualization, Conceptualization. **Mei Cui:** Writing – review & editing, Methodology, Conceptualization. **Jin-Tai Yu:** Writing – review & editing, Visualization, Funding acquisition, Data curation, Conceptualization.

Acknowledgements

The authors want to acknowledge the study participants and all the investigators involved in Alzheimer's Disease Neuroimaging Initiative (ADNI) for their helpful contributions to data collection. Data used in preparation for this paper were obtained from the ADNI database (http://adni.loni.usc.edu/). As such, the investigators within the ADNI contributed to the design and implementation of ADNI and/or provided data but did not participate in analysis or writing of this report. A complete listing of ADNI investigators can be found at: http://adni.loni.usc.edu/wp-content/uploads/how_to_apply/ADNI_Acknowledgement_List.pdf.

Supplementary materials

Supplementary material associated with this article can be found, in the online version, at doi:10.1016/j.tjpad.2024.100037.

References

[1] Wimo A, Seeher K, Cataldi R, et al. The worldwide costs of dementia in 2019. Alzheimer Dement 2023;19(7):2865–73. doi:10.1002/alz.12901.
[2] Jack CR Jr, Andrews JS, Beach TG, et al. Revised criteria for diagnosis and staging of Alzheimer's disease: Alzheimer's Association Workgroup. Alzheimer Dement 2024. doi:10.1002/alz.13859.
[3] Zanon Zotin MC, Yilmaz P, Sveikata L, et al. Peak width of skeletonized mean diffusivity: a neuroimaging marker for white matter injury. Radiology 2023;306(3):e212780. doi:10.1148/radiol.212780.
[4] Baykara E, Gesierich B, Adam R, et al. A novel imaging marker for small vessel disease based on skeletonization of white matter tracts and diffusion histograms. Ann Neurol 2016;80(4):581–92. doi:10.1002/ana.24758.
[5] Rasing I, Vlegels N, Schipper MR, et al. Microstructural white matter damage on MRI is associated with disease severity in Dutch-type cerebral amyloid angiopathy. J Cereb Blood Flow Metab 2024 271678x241261771. doi:10.1177/0271678x241261771.
[6] Chylińska M, Karaszewski B, Komendziński J, et al. Skeletonized mean diffusivity and neuropsychological performance in relapsing-remitting multiple sclerosis. Brain Behav 2022;12(6):e2591. doi:10.1002/brb3.2591.
[7] Jacob MA, Cai M, Bergkamp M, et al. Cerebral small vessel disease progression increases risk of incident Parkinsonism. Ann Neurol 2023;93(6):1130–41. doi:10.1002/ana.26615.
[8] Perosa V, Zanon Zotin MC, Schoemaker D, et al. Association between hippocampal volumes and cognition in cerebral amyloid angiopathy. Neurology 2024;102(2):e207854. doi:10.1212/wnl.0000000000207854.
[9] Durrani R, Wang M, Cox E, et al. Mediators of cognitive impairment in cerebral amyloid angiopathy. Int J Stroke 2023;18(1):78–84. doi:10.1177/17474930221099352.
[10] Petersen RC, Aisen PS, Beckett LA, et al. Alzheimer's Disease Neuroimaging Initiative (ADNI): clinical characterization. Neurology 2010;74(3):201–9. doi:10.1212/WNL.0b013e3181cb3e25.
[11] Tournier JD, Smith R, Raffelt D, et al. MRtrix3: a fast, flexible and open software framework for medical image processing and visualisation. Neuroimage 2019;202:116137. doi:10.1016/j.neuroimage.2019.116137.
[12] Smith SM, Jenkinson M, Woolrich MW, et al. Advances in functional and structural MR image analysis and implementation as FSL. Neuroimage 2004;23(Suppl 1):S208–19. doi:10.1016/j.neuroimage.2004.07.051.
[13] Moscoso A, Grothe MJ, Ashton NJ, et al. Longitudinal associations of blood phosphorylated tau181 and neurofilament light chain with neurodegeneration in Alzheimer disease. JAMA Neurol 2021;78(4):396–406. doi:10.1001/jamaneurol.2020.4986.
[14] Huang SY, Zhang YR, Guo Y, et al. Glymphatic system dysfunction predicts amyloid deposition, neurodegeneration, and clinical progression in Alzheimer's disease. Alzheimer Dement 2024;20(5):3251–69. doi:10.1002/alz.13789.
[15] Landau SM, Harvey D, Madison CM, et al. Comparing predictors of conversion and decline in mild cognitive impairment. Neurology 2010;75(3):230–8. doi:10.1212/WNL.0b013e3181e8e8b8.
[16] Palmqvist S, Mattsson N, Hansson O. Cerebrospinal fluid analysis detects cerebral amyloid-β accumulation earlier than positron emission tomography. Brain 2016;139(Pt 4):1226–36. doi:10.1093/brain/aww015.
[17] Landau SM, Fero A, Baker SL, et al. Measurement of longitudinal β-amyloid change with 18F-florbetapir PET and standardized uptake value ratios. J Nucl Med: Off Public Soc Nucl Med. 2015;56(4):567–74. doi:10.2967/jnumed.114.148981.
[18] Ossenkoppele R, Rabinovici GD, Smith R, et al. Discriminative accuracy of [18F]flortaucipir positron emission tomography for Alzheimer Disease vs other neurodegenerative disorders. JAMA 2018;320(11):1151–62. doi:10.1001/jama.2018.12917.
[19] Meyer PF, Pichet Binette A, Gonneaud J, Breitner JCS, Villeneuve S. Characterization of Alzheimer disease biomarker discrepancies using cerebrospinal fluid phosphorylated tau and AV1451 positron emission tomography. JAMA Neurol 2020;77(4):508–16. doi:10.1001/jamaneurol.2019.4749.
[20] Landau SM, Mintun MA, Joshi AD, et al. Amyloid deposition, hypometabolism, and longitudinal cognitive decline. Ann Neurol 2012;72(4):578–86. doi:10.1002/ana.23650.
[21] Bittner T, Zetterberg H, Teunissen CE, et al. Technical performance of a novel, fully automated electrochemiluminescence immunoassay for the quantitation of β-amyloid (1-42) in human cerebrospinal fluid. Alzheimer Dement 2016;12(5):517–26. doi:10.1016/j.jalz.2015.09.009.
[22] Schindler SE, Gray JD, Gordon BA, et al. Cerebrospinal fluid biomarkers measured by Elecsys assays compared to amyloid imaging. Alzheimer Dement 2018;14(11):1460–9. doi:10.1016/j.jalz.2018.01.013.
[23] Mattsson N, Cullen NC, Andreasson U, Zetterberg H, Blennow K. Association between longitudinal plasma neurofilament light and neurodegeneration in patients with Alzheimer disease. JAMA Neurol 2019;76(7):791–9. doi:10.1001/jamaneurol.2019.0765.
[24] Qiu T, Liu ZQ, Rheault F, et al. Structural white matter properties and cognitive resilience to tau pathology. Alzheimer Dement 2024;20(5):3364–77. doi:10.1002/alz.13776.
[25] Raposo N, Zanon Zotin MC, Schoemaker D, et al. Peak width of skeletonized mean diffusivity as neuroimaging biomarker in cerebral amyloid angiopathy. AJNR Am J Neuroradiol 2021;42(5):875–81. doi:10.3174/ajnr.A7042.
[26] McCreary CR, Beaudin AE, Subotic A, et al. Cross-sectional and longitudinal differences in peak skeletonized white matter mean diffusivity in cerebral amyloid angiopathy. Neuroimage Clin 2020;27:102280. doi:10.1016/j.nicl.2020.102280.
[27] Lam BYK, Leung KT, Yiu B, et al. Peak width of skeletonized mean diffusivity and its association with age-related cognitive alterations and vascular risk factors. Alzheimer Dement (Amst) 2019;11:721–9. doi:10.1016/j.dadm.2019.09.003.
[28] Low A, Mak E, Stefaniak JD, et al. Peak width of skeletonized mean diffusivity as a marker of diffuse cerebrovascular damage. Front Neurosci 2020;14:238. doi:10.3389/fnins.2020.00238.
[29] Frey BM, Petersen M, Schlemm E, et al. White matter integrity and structural brain network topology in cerebral small vessel disease: the Hamburg city health study. Hum Brain Mapp 2021;42(5):1406–15. doi:10.1002/hbm.25301.
[30] Mayo CD, Garcia-Barrera MA, Mazerolle EL, Ritchie LJ, Fisk JD, Gawryluk JR. Relationship between DTI metrics and cognitive function in Alzheimer's disease. Front Aging Neurosci 2018;10:436. doi:10.3389/fnagi.2018.00436.
[31] Kantarci K, Murray ME, Schwarz CG, et al. White-matter integrity on DTI and the pathologic staging of Alzheimer's disease. Neurobiol Aging 2017;56:172–9. doi:10.1016/j.neurobiolaging.2017.04.024.
[32] Amlien IK, Fjell AM. Diffusion tensor imaging of white matter degeneration in Alzheimer's disease and mild cognitive impairment. Neuroscience 2014;276:206–15. doi:10.1016/j.neuroscience.2014.02.017.

[33] Douaud G, Jbabdi S, Behrens TE, et al. DTI measures in crossing-fibre areas: increased diffusion anisotropy reveals early white matter alteration in MCI and mild Alzheimer's disease. Neuroimage 2011;55(3):880–90. doi:10.1016/j.neuroimage.2010.12.008.
[34] Brueggen K, Grothe MJ, Dyrba M, et al. The European DTI study on dementia - a multicenter DTI and MRI study on Alzheimer's disease and mild cognitive impairment. Neuroimage 2017;144(Pt B):305–8. doi:10.1016/j.neuroimage.2016.03.067.
[35] Oberlin LE, Respino M, Victoria L, et al. Late-life depression accentuates cognitive weaknesses in older adults with small vessel disease. Neuropsychopharmacology 2022;47(2):580–7. doi:10.1038/s41386-021-00973-z.
[36] Tang X, Qin Y, Zhu W, Miller MI. Surface-based vertexwise analysis of morphometry and microstructural integrity for white matter tracts in diffusion tensor imaging: with application to the corpus callosum in Alzheimer's disease. Hum Brain Mapp 2017;38(4):1875–93. doi:10.1002/hbm.23491.
[37] Kumar S, De Luca A, Leemans A, et al. Topology of diffusion changes in corpus callosum in Alzheimer's disease: an exploratory case-control study. Front Neurol 2022;13:1005406. doi:10.3389/fneur.2022.1005406.
[38] Liu X, Du L, Zhang B, et al. Alterations and associations between magnetic susceptibility of the basal Ganglia and diffusion properties in Alzheimer's disease. Front Neurosci 2021;15:616163. doi:10.3389/fnins.2021.616163.
[39] Chen Y, Wang Y, Song Z, Fan Y, Gao T, Tang X. Abnormal white matter changes in Alzheimer's disease based on diffusion tensor imaging: a systematic review. Ageing Res. Rev. 2023;87:101911. doi:10.1016/j.arr.2023.101911.
[40] Moll NM, Rietsch AM, Thomas S, et al. Multiple sclerosis normal-appearing white matter: pathology-imaging correlations. Ann Neurol 2011;70(5):764–73. doi:10.1002/ana.22521.
[41] van Veluw SJ, Reijmer YD, van der Kouwe AJ, et al. Histopathology of diffusion imaging abnormalities in cerebral amyloid angiopathy. Neurology 2019;92(9):e933–ee43. doi:10.1212/wnl.0000000000007005.
[42] Hillmer L, Erhardt EB, Caprihan A, et al. Blood-brain barrier disruption measured by albumin index correlates with inflammatory fluid biomarkers. J Cereb Blood Flow Metab 2023;43(5):712–21. doi:10.1177/0271678x221146127.
[43] Jack CR Jr, Knopman DS, Jagust WJ, et al. Hypothetical model of dynamic biomarkers of the Alzheimer's pathological cascade. The Lancet Neurology 2010;9(1):119–28. doi:10.1016/s1474-4422(09)70299-6.
[44] Sepulcre J, Sabuncu MR, Becker A, Sperling R, Johnson KA. In vivo characterization of the early states of the amyloid-beta network. Brain 2013;136(Pt 7):2239–52. doi:10.1093/brain/awt146.
[45] Garnier-Crussard A, Cotton F, Krolak-Salmon P, Chételat G. White matter hyperintensities in Alzheimer's disease: beyond vascular contribution. Alzheimer Dement 2023;19(8):3738–48. doi:10.1002/alz.13057.
[46] Prins ND, Scheltens P. White matter hyperintensities, cognitive impairment and dementia: an update. Nat Rev Neurol 2015;11(3):157–65. doi:10.1038/nrneurol.2015.10.
[47] Garnier-Crussard A, Bougacha S, Wirth M, et al. White matter hyperintensity topography in Alzheimer's disease and links to cognition. Alzheimer Dement 2022;18(3):422–33. doi:10.1002/alz.12410.
[48] McAleese KE, Miah M, Graham S, et al. Frontal white matter lesions in Alzheimer's disease are associated with both small vessel disease and AD-associated cortical pathology. Acta Neuropathol 2021;142(6):937–50. doi:10.1007/s00401-021-02376-2.